โครงการ

การเรียนการสอนเพื่อเสริมประสบการณ์

ชื่อโครงการ การศึกษาโดยวิธีพลวัตเชิงโมเลกุลของสารกลุ่มฟิวโรฟิวแรนลิกแนนซึ่งเป็นสารยับยั้งในยาต้านโรคเบาหวาน

A molecular dynamics study of furofuran lignans as an inhibitor of antidiabetic drug target

ชื่อนิสิต นายพิสิฐ เลิศธนะกิจ เลขประจำตัว 5933078723

ภาควิชา เคมี

ปีการศึกษา 2562

คณะวิทยาศาสตร์ จุฬาลงกรณ์มหาวิทยาลัย

การศึกษาโดยวิธีพลวัตเชิงโมเลกุลของสารกลุ่มฟิวโรฟิวแรนลิกแนนซึ่งเป็นสารยับยั้งในยาต้านโรคเบาหวาน

A molecular dynamics study of furofuran lignans as an inhibitor of antidiabetic drug target

โดย

นายพิสิฐ เลิศธนะกิจ

รายงานชิ้นนี้เป็นส่วนหนึ่งของการศึกษาตามหลักสูตร

ปริญญาวิทยาศาสตรบัณฑิต

ภาควิชาเคมี คณะวิทยาศาตร์

จุฬาลงกรณ์มหาวิทยาลัย

ปีการศึกษา 2562

A molecular dynamic study of furofuran lignans as an inhibitor of antidiabetic drug target

Mr. Pisit Lerttanakij

In Partially fulfillment for the Degree of Bachelor of Science

Department of Chemistry, Faculty of Science

Chulalongkorn University

Academic Year 2019

Project Title: A molecular dynamics study of furofuran lignans as an inhibitor of antidiabetic drug target

Student Name: Mr. Pisit Lerttanakij

Accepted by Department of Chemistry, Faculty of science, Chulalongkorn University in Partial fulfillment of the Requirement for the Degree of Bachelor of Science

Senior Project Committee

1. Professor Dr. Khanitha Pudhom	Chair Committee
2. Associate Professor Dr. Somsak Pianwanit	Committee
3. Professor Dr. Pornthep Sompornpisut	Project Advisor
4. Associate Professor Dr. Preecha Phuwapraisirisan	Project Co-advisor

This report was approved by head of Department of Chemistry

.....

(Professor Dr. Pornthep Sompornpisut, Ph.D.)

Project Advisor

.....

(Associate Professor Dr. Vudhichai Parasuk, Ph.D.)

Head of Department of Chemistry

Preecha Phuwapraisirisan

.....

(Associate Professor Preecha Phuwapraisirisan, Ph.D.)

Project Co-advisor

Date 10 Month June Year 2020

ชื่อโครงการ การศึกษาโดยวิธีพลวัตเชิงโมเลกุลของสารกลุ่มฟิวโรฟิวแรนลิกแนนซึ่งเป็นสารยับยั้งในยาต้านโรคเบาหวาน

ชื่อนิสิตในโครงการ นายพิสิฐ เลิศธนะกิจ **เลขประจำตัว** 5933078723

ชื่ออาจารย์ที่ปรึกษา ศาสตราจารย์ ดร.พรเทพ สมพรพิสุทธิ์

ชื่ออาจารย์ที่ปรึกษาร่วม รองศาสตราจารย์ ดร.ปรีชา ภูวไพรศิริศาล

ภาควิชาเคมี คณะวิทยาศาสตร์ จุฬาลงกรณ์มหาวิทยาลัย ปีการศึกษา 2562

บทคัดย่อ

มีรายงานวิจัยค้นพบสารประกอบในกลุ่มฟิวโรฟิวแรนลิกแนนสามารถทำหน้าที่เป็นสารยับยั้งเอนไซม์แอลฟา-กลูโคสิเดส การศึกษานี้ใช้วิธีการเข้าจับเชิงโมเลกุลและการจำลองพลวัติเชิงโมเลกุลเพื่อตรวจสอบอันตรกิริยาระหว่างสารยับยั้งในกลุ่มฟิวโรฟิวแรนลิกแนนกับเอนไซม์มอลเทสจากมนุษย์ ในการจำลองระบบได้เลือกสารประกอบในกลุ่มนี้จำนวน 4 ชนิดได้แก่ α-8b, α-14, β-14 และสารประกอบหมายเลข 4 และใช้แบบจำลองของอะคาร์โบสกับเอนไซม์มอลเทสเป็นการทดลองควบคุมและเปรียบเทียบ ผลการคำนวณพบว่าลักษณะการเข้าจับของสารประกอบทั้ง 4 มีลักษณะคล้ายกับอะคาร์โบส โดยใช้หมู่ 3,4-dihydroxyphenyl หันเข้าบริเวณยึดจับและสร้างพันธะไฮโดรเจนกับกรดอะมิโนของเอนไซม์ อย่างไรก็ตาม พบว่าโมเลกุลของน้ำในโครงผลึกช่วยเพิ่มความเสถียรของสารยับยั้งในบริเวณยึดจับ จากผลการคำนวณ ค่าพลังงานเสรีของการยึดจับระหว่างสารยับยั้งกับเอนไซม์มอลเทสเรียงตามลำดับดังนี้ maltase-β-14 > maltase-α-14 > maltase-α-8b ซึ่งสอดคล้องกับค่า IC50 ที่ได้จากการทดลอง

คำสำคัญ: ฟิวโรฟิวแรนลิกแนน, วิธีพลวัตเชิงโมเลกุล, แอลฟา-กลูโคสิเดส

Project Title A molecular dynamics study of furofuran lignans as an inhibitor of antidiabetic drug target

Student Name Mr. Pisit Lerttanakij **Student ID** 5933078723

Advisor Name Professor Pornthep Sompornpisut. Ph.D.

Co-advisor Name Associate Professor Vudhichai Parasuk. Ph.D.

Department of Chemistry, Faculty of Science, Chulalongkorn University, Academic Year 2019

Abstract

An earlier research study has found that furofuran type lignans have exhibited an alpha-glucosidase inhibition. In this study, molecular docking and molecular dynamics simulation were carried out to investigate the interaction between furofuran lignan derivatives and human maltase. In the system simulation, four compounds were chosen, namely **α**-8b, **α**-14, **β**-14 and compound 4. The simulation of the maltase-acarbose model system was used as a control study and comparison. The results showed that the binding characteristics of all 4 compounds were similar to that of acarbose by orienting the 3,4-dihydroxyphenyl group towards the binding pocket and forming the hydrogen bonds with the amino acid residues within the binding site. However, the water molecules in the crystal structure were found to enhance the stability of the inhibitors in the binding site. From the calculated results, the free energies of the binding between the inhibitors and the maltase were in the following order: maltase-**β**-14 > maltase-**α**-14 > maltase-**α**-8b, which is consistent with the experimentally-determined IC_{50} values.

Keywords: Furofuran lignans, Molecular dynamic, **α**-glucosidase

ACKNOWLEDGEMENTS

Firstly, I would like to thank my advisor, Professor Dr. Pornthep Sompornpisut and my co-advisor, Associate Professor Dr. Preecha Phuwapraisirisan for his support and advice, which helped me in doing project and I came to know about so many new things.

I would also like to thank my project committee, Professor Dr. Khanitha Pudhom and Associate Professor Dr. Somsak Pianwanit for offering their time, support, suggestion and review of this document.

I would like to all members of Computational Chemistry Unit Cell (CCUC) for their kindness and friendliness over the time of doing project.

The Scholarship from The Development and Promotion of Science and Technology Talents Project (DPST).

Finally, I would like to thank my family for great support to me.

TABLE OF CONTENTS

LIST OF TABLES

LIST OF FIGURES

Chapter 1

INTRODUCTION

1.1 Diabetes mellitus (DM)

Diabetes mellitus, also known as diabetes, is a metabolic disorder disease that causes an excessive amount of sugar in blood so-called hyperglycemia. Hyperglycemia condition is a consequence of deficiency of insulin secretion or resistance to insulin action, or both[1].

Insulin is a hormone produced in the pancreas. Insulin acts to control the sugar level in the body. The amount of insulin is regulated by the sugar level in blood. When blood sugar level is high, the pancreas releases insulin to circulatory system. Then, insulin binds to the insulin receptor and allow glucose to be transported into the cells. The homeostatic mechanism for insulin regulation of blood glucose levels is shown in Figure 1.1.

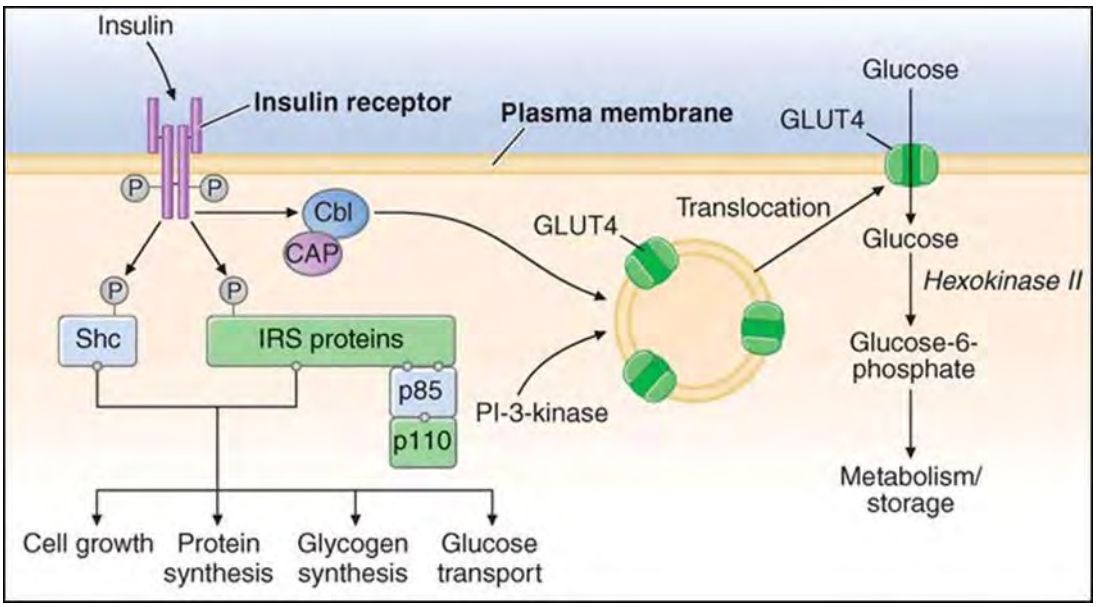

Figure 1.1 Mechanism of action of insulin[2].

The deficiency of insulin action leads to several abnormal metabolisms. Diabetes patients may suffer from failure of various organs that leads to severe health conditions such as cardiovascular disease, nerve damage, kidney damage, eye damage, foot damage, skin conditions, hearing impairment, Alzheimer's disease, and depression. Although several

pathogenic processes may be involved in the development of diabetes, it can be classified into two major categories: type 1 and type 2 diabetes [3].

Type 1 DM is characterized by an autoimmune destruction of pancreatic β-cell followed by an insulin deficiency (Figure 1.2). This type of DM comprises approximately 5 to 10 percent of all diabetes patients. Type 1 DM patients can be treated by insulin injection to compensate insulin deficientcy[4].

Type 2 DM is characterized by insulin resistance, hyperinsulinemia and eventually by β-cell failure (Figure 1.2). Type 2 DM makes up 90 percent of all diabetes patients[5]. The cause of type 2 DM depends on several factors, including lifestyle and genes. Obesity is the most common health conditions in type 2 DM. It comprises approximately 50 to 90 percent of diabetes patients with type 2 DM[6, 7]. The global diabetes prevalence in 2019 is about 9.3 percent (463 million people) with an increasing number at alarming rate [8]. Type 2 DM has been accounted for approximately 90 percent of total.

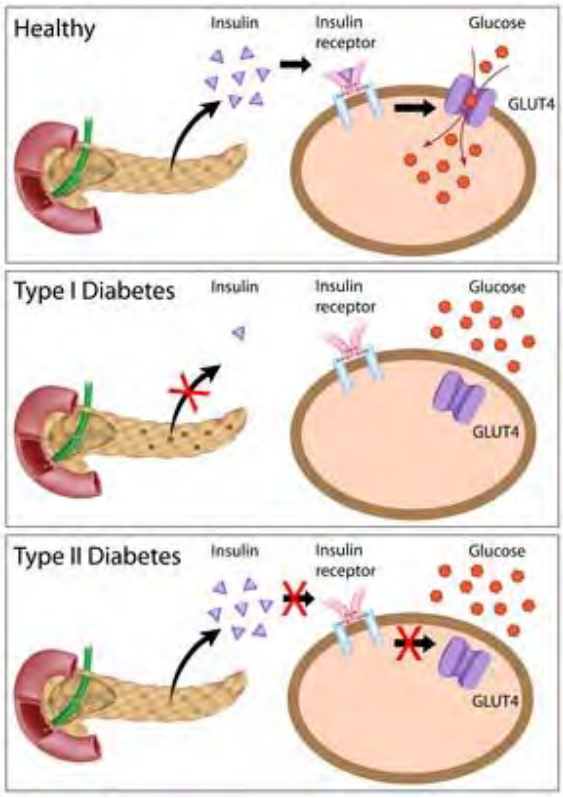

Figure 1.2 Type 1 DM and Type 2 DM. (https://www.wonderopolis.org/)

Type 2 DM can be treated in a several approaches. Each approach works in different ways to lower blood sugar level. One of many approaches is to delay the hyperglycemia by reducing the rate of carbohydrate digestion through the inhibition of α-glucosidase[9].

1.2 Type of inhibition

The inhibition mechanism can be classified into 3 types: competitive inhibition, non-competitive inhibition and uncompetitive inhibition.

In competitive inhibition, the inhibitor binds in the same binding site as the substrate. In this type of inhibition, the inhibitor and substrate compete each other to bind in the same bonding site. Once the inhibitor is bound in the binding pocket, it prevents the substrate from binding. The mechanism of the competitive inhibition is shown in Figure 1.3.

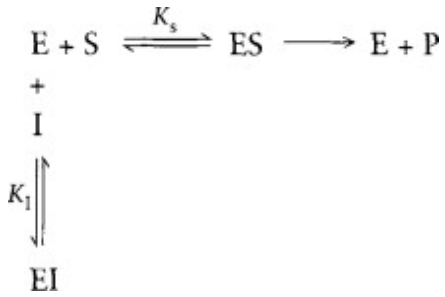

Figure 1.3 The mechanism of competitive inhibition[10].

Noncompetitive inhibition has a mechanism different from the competitive inhibitor, in a way that the binding region of the inhibitor is not the same as the substrate. Therefore, noncompetitive inhibitor can bind to the enzyme with or without substrate. The enzyme-substrate-inhibitor complex cannot give any product. The mechanism of noncompetitive is shown in Figure 1.4.

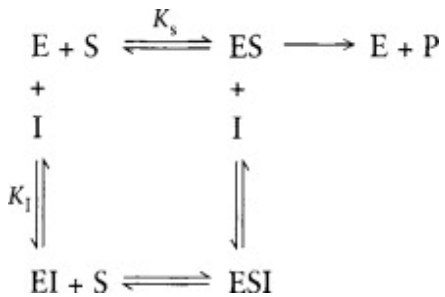

Figure 1.4 The mechanism of noncompetitive inhibition[10].

Uncompetitive inhibition is similar to noncompetitive inhibition, but the uncompetitive inhibitor can bind with only the enzyme-substrate complex and form the enzyme-substrate-inhibitor complex that cannot give any product. The mechanism of uncompetitive is shown in Figure 1.5.

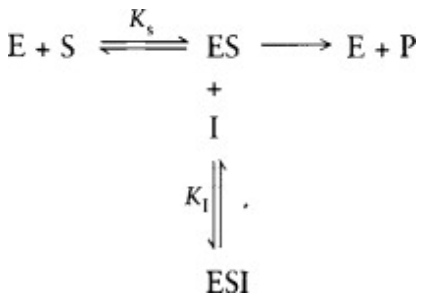

Figure 1.5 The mechanism of uncompetitive inhibition[10].

1.3 α-Glucosidase inhibitor

α-Glucosidase is an enzyme that selectively hydrolyzes terminal non-reducing (1→4)-linked α-glucose residue of carbohydrate (Figure 1.6). α-Glucosidase is located in the brush border of the small intestine. Inhibition of α-glucosidase can reduce rate of hydrolysis and delay glucose absorption of small intestine, resulting in the lower blood glucose levels after eating. Currently, acarbose, which is the an competitive inhibitor of α-glucosidase, is used as antidiabetic drug.

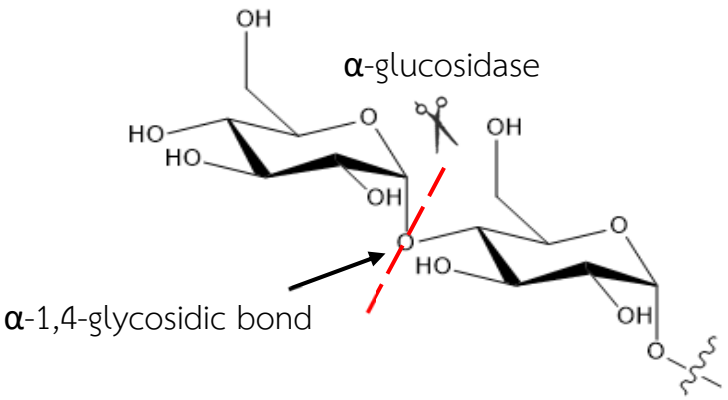

Figure 1.6 The hydrolytic reaction at the α-1,4-glycosidic bond of oligosaccharide by α-glucosidase.

Acarbose (Precose®, Pandrase® or Glucobay®) is an orally antidiabetic agent that is commercially available[11]. Acarbose is a pseudotetrasaccharide containing a 4-amino-4,6-dideoxy-glucose unit connected with two glucose residues (Figure 1.7). Acarbose contains a non-hydrolyzable nitrogen-linked bond that competitively inhibits α-amylase activity. Acarbose was first isolated from bacteria *Actinoplanaes* sp. Acarbose acts as a strong competitive inhibitor against α-glucosidase. However, long-term drug administration has led to several side effects such as flatulence, bloating, diarrhea and soft stools[12]. Therefore, developing effective drugs with fewer side effects for diabetes patients has become the subject of attention

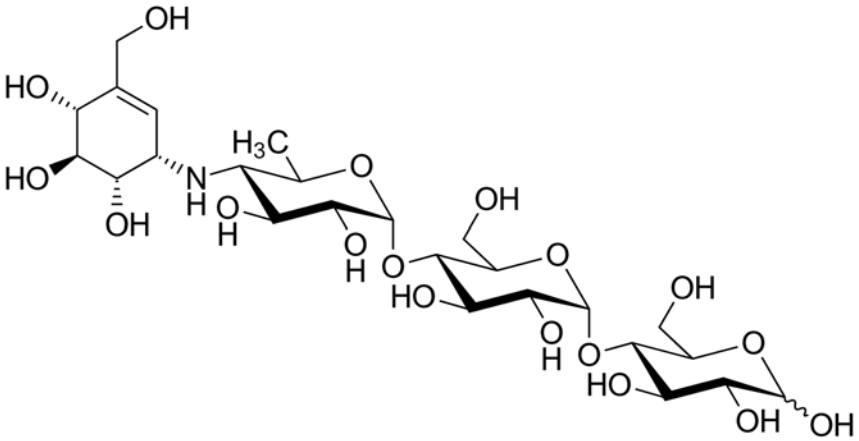

Figure 1.7 Structure of acarbose containing a non-hydrolyzable nitrogen-linked bond.

In 2006, Pullela and co-workers extracted and isolated compounds from *Piper longum*[13]. There are five compounds, which are pipataline, pellitorine, sesamine, brachystamide B, and guineensine (Figure 1.8), and inhibitory activity against α-glucosidase was also evaluated. The half maximal inhibitory concentration (IC_{50}) of pipataline, pellitorine, sesamine, brachystamide B, and guineensine were 30.10, 34.39, 36.39, 34.09, and 19.26 mM [14], respectively.

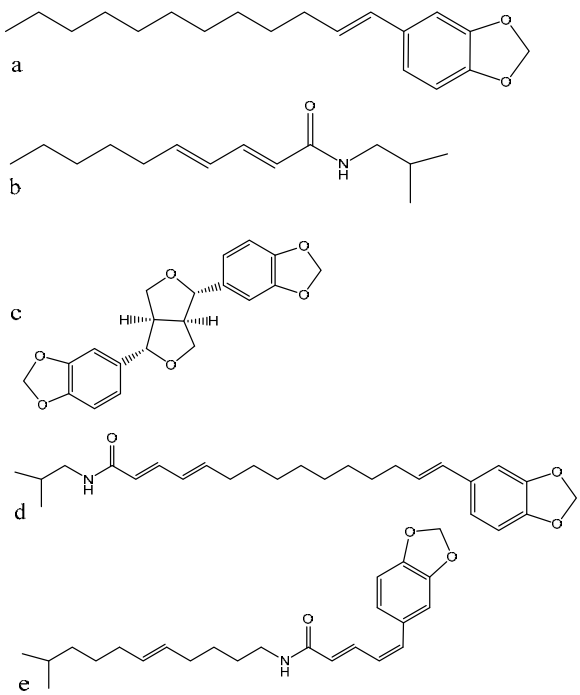

Figure 1.8 structures of (a) pipataline, (b) pellitorine, (c) sesamine, (d) brachystamide B and (e) guineensine.

Sesamine is a furofuran lignan, which is one of the largest sub-type of classical lignans and classified by a 2,6-diraryl-3,7-dioxabicyclo[3.3.0]octane motif that contain a variety of aromatic substituents at C2 and C6 of 3,7-dioxabicyclic core[15] (Figure 1.9).

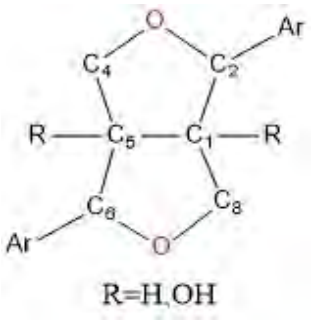

Figure 1.9 General structure of furofuran lignan.

In 2019, Worawalai and co-workers synthesized a series of furofuran lignan derivatives that were found to exhibit a remarkable inhibitory effect against baker's yeast and rat intestinal α-glucosidases[16]. From the enzyme kinetic study α-8b, α-14, β-14, and compound 4 (Figure 1.10) have been shown to be potent inhibitors in both competitive and non-competitive mechanisms. In their study, interactions between the protein and these compounds have

been investigated in non-competitive mode using a molecular modeling study. To gain a complete picture of the inhibitory activity, a molecular dynamics (MD) simulation study on binding of the furofuran lignan derivatives to maltase-glucoamylase was carried out in the competitive type of inhibition. This study provides insight into the binding pattern of antidiabetic α-glucosidase inhibitors within the active site of the protein.

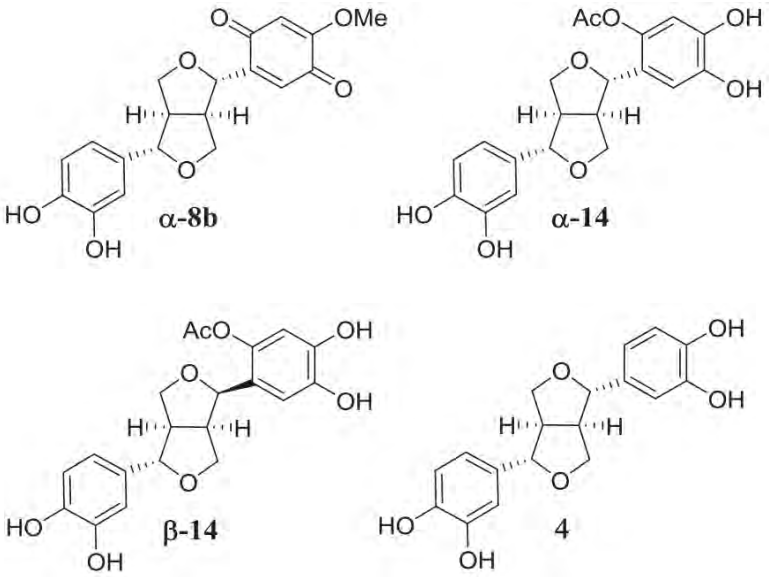

Figure 1.10 Structures of α-8b, α-14, β-14, and compound 4.

1.4 Molecular dynamic simulation

Molecular dynamic (MD) simulation has been shown to be a powerful tool for investigating interactions between protein and ligand. MD provides insight into an important region of the active site involved in the binding of the inhibitor.

1.4.1 The Newton's Second Law

MD simulation is relied on solving the numerical integration of the second law of Newton's equation of motion [17]. This technique generates the motion of particles as a function of time by taking into account physical interactions between particles present in the system. From the Newton's second law (Eq. 1.1), a force acting on particle i^{th} F_i can be described as a product of an acceleration a_i and its mass m_i. Acceleration in the equation 1.2 can be defined as the second derivative of position r_i with respect to a change in time or the first derivative

of velocities v_i over time (equation 1.3). The force acting on any particles is calculated by the gradient or the first derivative of the potential energy (U) with respect to the position change (equation 1.4). Particle positions and velocities of each particle are determined by specific inter-atomic potential energy and temperature-defined kinetic energy, respectively. During MD simulation, successive configurations are called dynamic trajectory which is composed of time-dependent positions and velocities of the particles in the system.

$$F_i = m_i a_i \tag{1.1}$$

$$\frac{d^2 r_i}{dt^2} = \frac{F_i}{m_i} \tag{1.2}$$

$$\frac{dv_i}{dt} = \frac{F_i}{m_i} \tag{1.3}$$

$$F_i = -\frac{\partial U}{\partial r_i} \tag{1.4}$$

1.4.2 Molecular mechanical force field

In molecular mechanic theory, the potential energy of the system is a function of atomic position. Atomistic models considered as sphere are connected with bonds as springs. Atoms that are greater than two bonds apart can interact through van der Waals attraction, steric repulsion, and electrostatic attraction/repulsion. The potential energy can be described by the sum of individual two-body interacting terms[18, 19]. A general form of the molecular mechanic potential function is show in equation 1.5.

$$U = \sum_{bond} k_b (r-r_0)^2 + \sum_{angle} k_\theta (\theta-\theta_0)^2 + \sum_{torsion} k_\varphi \left[1+\cos\left(n\varphi+\delta\right)\right] + \sum_{improper} k_\psi (\psi-\psi_0)^2$$
$$+ \sum_{vdW} \epsilon\left(\frac{A_{ij}}{r_{ij}^6} - \frac{B_{ij}}{r_{ij}^{12}}\right) + \sum_{elec} \frac{q_i q_j}{4\pi\varepsilon_0 r_{ij}} \tag{1.5}$$

Where k_b, k_θ, k_φ and k_ω refer to the force constant of the potential functions associated with bond stretching, angle, torsion angle, and improper torsion, respectively. The ϵ, A_{ij} and B_{ij} are

coefficient for Van der Waals term. The distance r_{ij} defines a separation between the particle i^{th} and j^{th} with partial atomic charge q_i and q_j.ε_0 is dielectric constant. The first four terms are used to calculate the bonded energy. The fifth term is known as the Lennard-Jones potential function. The last term is the electrostatic energy. All parameters defined in Eq 1.5 equation are called force-field parameters (Figure 1.11).

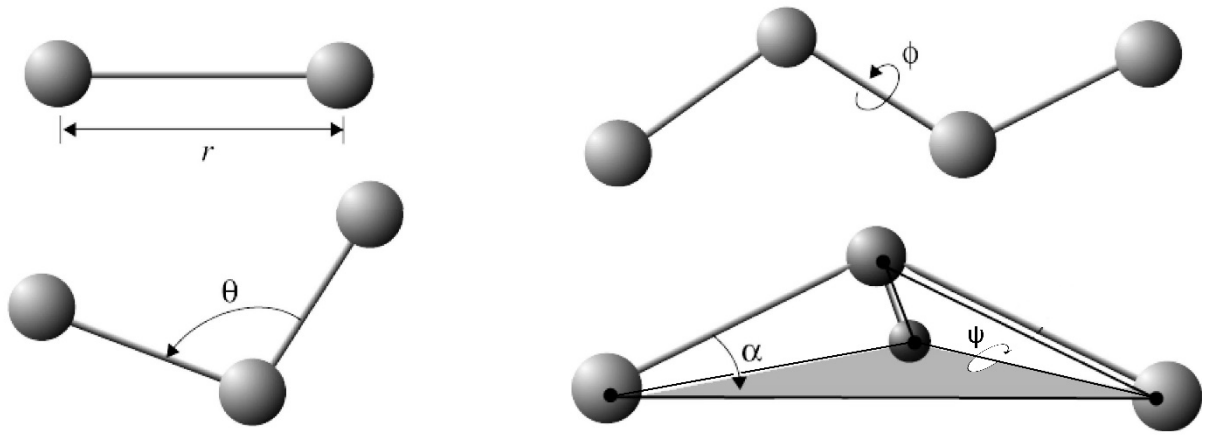

Figure 1.11 The force field interaction parameters: bond distance (r), bond angle (**θ**), torsion angle (**φ**), and improper torsion angle (**ψ**). (https://www.ks.uiuc.edu/)

1.5 Analysis from MD results[20, 21]

The trajectory generated by MD contains information that are typically used for a subsequent analysis to obtain meaningful structural as well as thermodynamical properties of the system such as root mean square deviation, hydrogen bond, and Gibbs free energy of binding.

1.5.1 The root mean square deviation (RMSD)

RMSD indicates how an investigating structure deviate from a reference one. RMSD is typically computed based on a comparison between atomic coordinates of a group of selected atoms or part of an investigating molecule and those of the same set of atoms of reference structure. RMSD of MD trajectory is generally calculated by taking structure

coordinates from MD snapshot and performing a least-square fitting least-square fitting method with the reference structure as shown equation 1.6.

$$\mathrm{RMSD}\left(t_i,t_j\right)=\left[\frac{1}{N}\sum_{n=1}^{N}\left\|r(t_j)-r(t_i)\right\|^2\right]^{\frac{1}{2}} \tag{1.6}$$

Where N is number of interested atoms and $r(t_i)$ and $r(t_j)$ is position of MD atom i and a reference atom j at time t.

1.5.2 The hydrogen bond

Hydrogen bonding provides significant interactions between protein and ligand. A hydrogen bonding in MD simulation is generally evaluated based on a structure geometry made by hydrogen bond donor (D) atoms and hydrogen bond acceptor (A) with a criterion of atoms distances (r) less than 3.5 Å and angles (**α**) less than 60° (Figure 1.12).

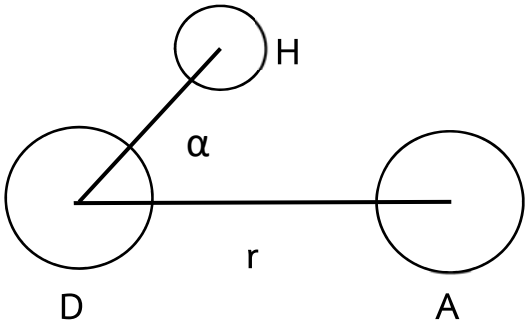

Figure 1.12 Criterion of Hydrogen bond geometry.

1.5.3 Gibbs free energy of binding

The molecular mechanics energies combined with the generalized Born and surface area continuum solvation (MM/GBSA) have been widely used acceptable method to estimate the free energy of binding (ΔG_{bind}) of receptor-ligand complexes. The binding free energy of the complex can be obtained based on a thermodynamic cycle of the free energy of solvation of receptor, ligand and its complex forms (Figure 1.13). The difference in the

solvation free energy of complex (ΔG_{cpx}) subtracted by that of protein (ΔG_{pro}) and ligand (ΔG_{lig}) results in the ΔG_{bind} as shown in equation 1.7.

$$\Delta G_{bind} = \Delta G_{cpx} - (\Delta G_{pro} + \Delta G_{lig}) \quad (1.7)$$

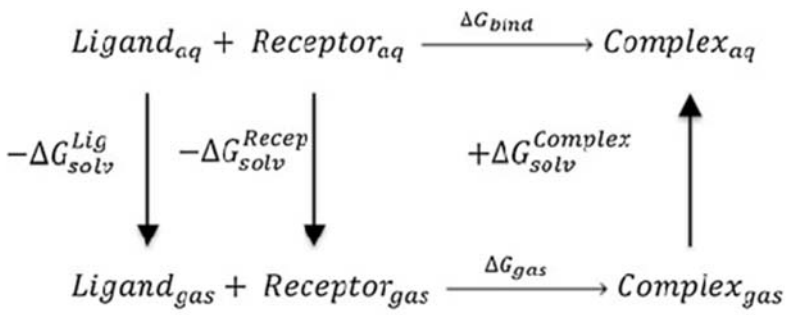

Figure 1.13 Thermodynamic cycle of free energy of binding calculation[22].

1.6 Objectives

To investigate the binding pose of the previously synthesized furofuran lignan derivatives to human maltase in the competitive mode of inhibition using a molecular modeling, molecular dynamic simulation and binding free energy.

Chapter 2

METHODOLOGY

2.1 Program

2.1.1 Discovery studio

Discovery studio is a software suite for visualization, molecular modeling and simulation of small molecule and macromolecule systems. This software package is also capable of conducting a molecular docking technique. In this study, the CDOCKER available in Discovery studio was used to optimize the orientation of inhibitors within the active site of the enzyme. Discovery studio has been developed and distributed by Dassault Systemes BIOVIA. (https://www.3dsbiovia.com/)

2.1.2 Visual Molecular Dynamics (VMD)[23, 24]

VMD is a program useful for molecular modeling and simulation study of biological molecules. It has been developed by Theoretical and Computational Biophysics Group at the Beckman Institute for Advanced Science and Technology, University of Illinois at Urbana–Champaign. (https://www.ks.uiuc.edu/Research/vmd/)

2.1.3 Nanoscale Molecular Dynamics (NAMD)[25]

NAMD is a program used to carry out molecular dynamic simulation and free energy calculations. It has been developed by the Theoretical and Computational Biophysics Group at the Beckman Institute for Advanced Science and Technology, The University of Illinois at Urbana-Champaign. (https://www.ks.uiuc.edu/Research/namd/)

2.1.4 The CHARMM force field[26]

The name “CHARMM” stands for Chemistry at Harvard Macromolecular Mechanics (CHARMM). CHARMM is known as a set of force field parameters used for molecular dynamics

simulation. The CHARMM force field parameters have been developed worldwide. The pioneer developers are Martin Karplus and his group at Harvard University.

2.2 computational method

2.2.1 system preparation

The model of the N-terminal subunit of human maltase-glucoamylase in complex with acarbose was taken from the crystal structure with Protein Data Bank (PDB) entry codes 2QMJ[27] (Figure 2.1). The 3D structures of four furofuran lignan inhibitors, including α-8b, α-14, β-14 and compound 4, (Figure 1.7) were taken from the previous publication[16]. Those inhibitor structures were obtained through geometric optimization vis quantum chemical calculation. Each inhibitor was docked into the binding pocket of the enzyme using CDOCKER (Figure 2.2). The binding pose was evaluated based on the interaction energy in terms of CDOCKER score. The enzyme-inhibitor models with the best score were subsequently refined using all atom MD simulation in explicit solvent.

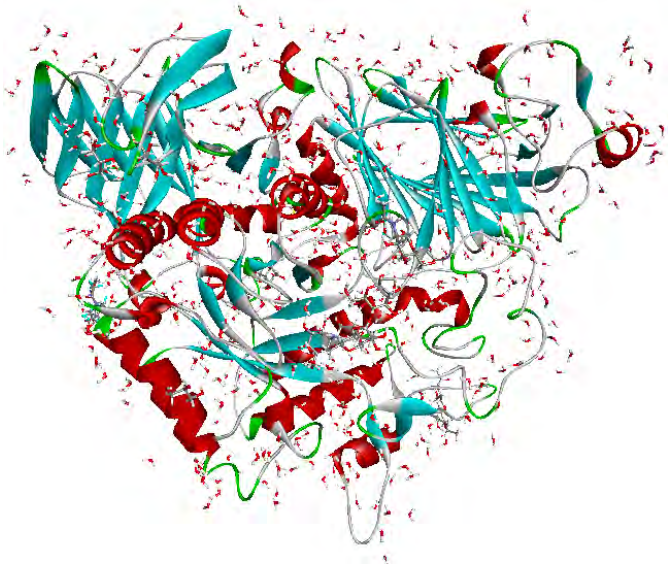

Figure 2.1 The crystal structure (2QMJ) of human maltase-glucoamylase (cartoon representation) in complex with acarbose (stick representation). Crystallographic waters surrounding the enzyme are also shown as a stick model.

Structure topology of the protein-inhibitor system for MD simulation was constructed based on the CHARMM36 topology. The structure topology of the inhibitors was generated using the CHARMM GUI webserver. Hydrogen atoms that were not present in the crystal structure were added. The addition of hydrogen atom was taken into account an ionization state of amino acid side chain at neutral pH. Each docked model was immersed in a 130x130x130 $Å^3$ box of water molecules. Then the protein charge was neutralized by an addition of counter-ions (NaCl) at a concentration of 0.1 M (Figure 2.3). At this step, the total number of atoms in the MD system is approximately 200,000 atoms. All the topology preparation steps were processed through the VMD program using TCL command scripts.

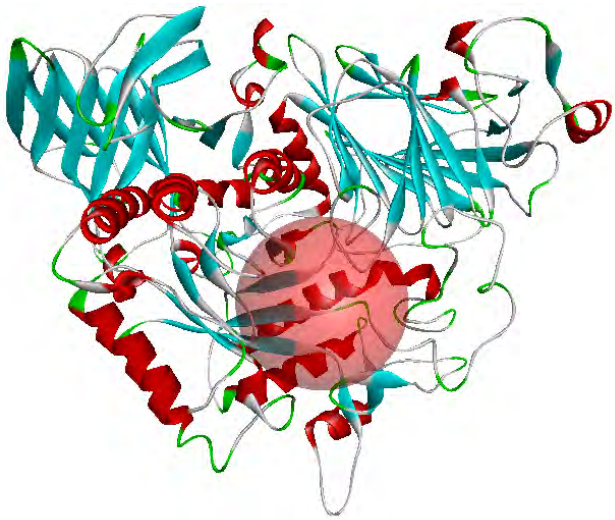

Figure 2.2 The active site of human intestinal maltase.

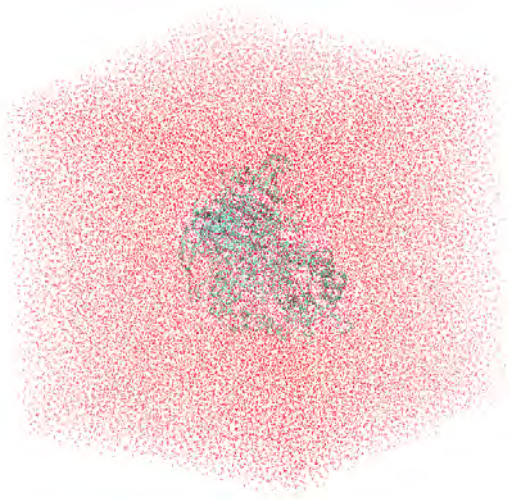

Figure 2.3 The system after solvation and neutralization.

2.2.2 Molecular dynamic simulation

MD simulations of all the protein-inhibitor systems were carried out using the NAMD2 program. The potential energy of the system was computed using the CHARMM36 force field for protein and counter-ions, TIP3P force field for water and CHARMM generalized force field for the inhibitors. The force field parameters for furofuran lignan inhibitors were obtained from the CHARMM GUI webserver. MD simulations were performed at 1 atm and 298 K with the isothermal-isobaric (NPT) ensemble. All systems were gradually relaxed by 20,000 steps of energy minimization for removing bad contacts and 20,000 steps of MD with constraining positions of protein and inhibitor atoms to attain a gradual increase in velocity in order to keep the stability of the system without steric crash. MD simulations were conducted with a time step of 2 fs (femtosecond). For a trajectory storage, the MD configurations and its velocities at every 2 ps (picosecond) were recorded. More than 100 ns (nanosecond) of MD simulations were performed for all systems. MD trajectories of each system were used for the analysis of structure and thermodynamic properties including molecular surface visualization, RMSD, hydrogen bonding and the binding free energy. The trajectory analysis was performed through the VMD program using TCL command scripts.

Chapter 3

RESULTS AND DISCUSSION

3.1 Molecular docking result

From the docking result, the structure of the lowest docking energy between human maltase and each inhibitor are shown in Figure 3.1

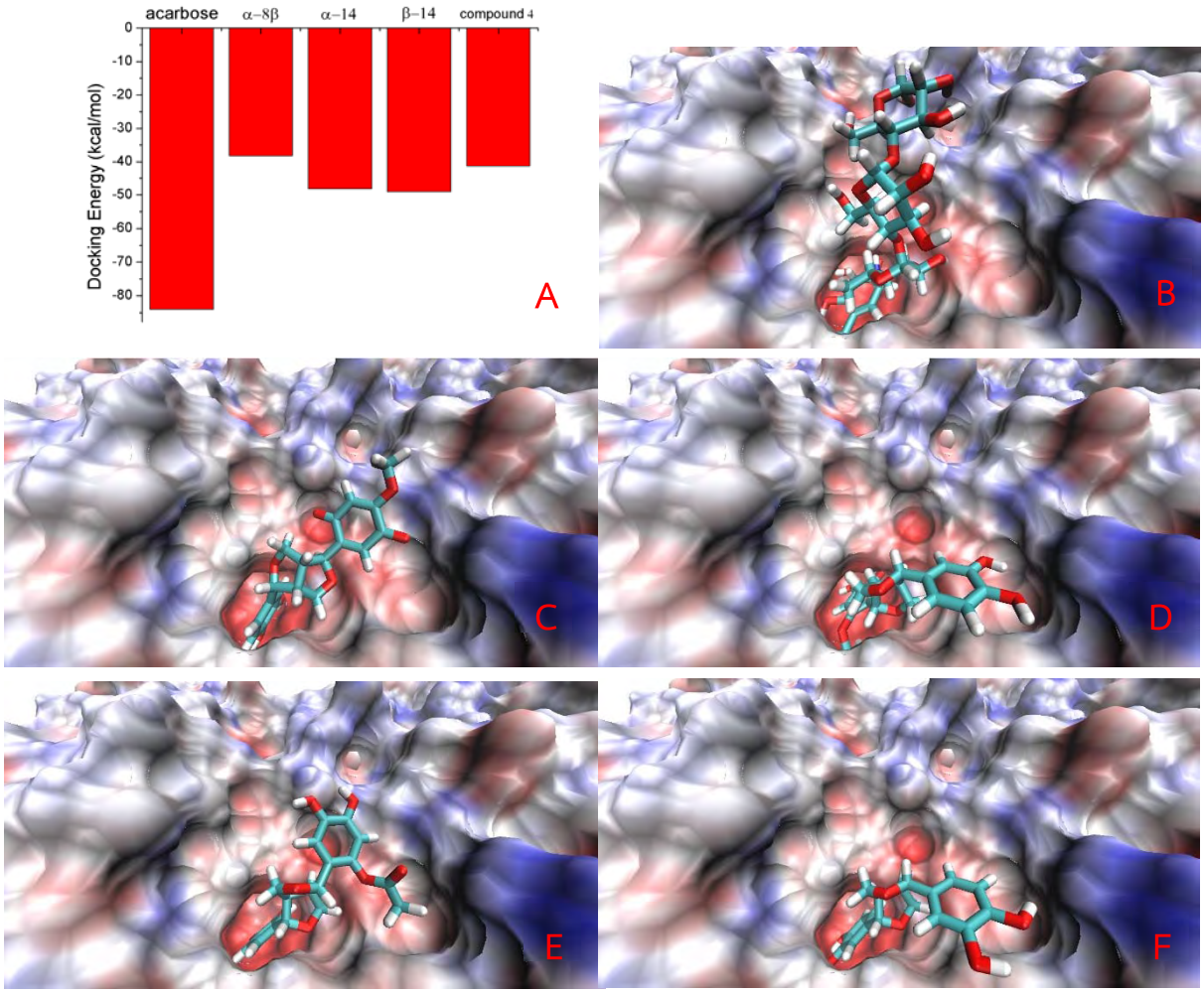

Figure 3.1 The docking energy (A) and the top-rank binding pose of the inhibitors in the active site of human maltase. The inhibitors, acarbose (B), α-8b (C), α-14 (D), β-14 (E) and compound 4 (F) are shown as stick model mapped onto electrostatic potential surface of the active site. The color indicates ranging from red, white and blue indicates negative, neutral and positive charges, respectively.

From the docking results , all furofuran lignans were found to bind in the active site of the enzyme in a very similar binding pose. This suggested similar binding interactions among the different compounds in the binding site. Furthermore, it appeared that α-8b, β-14 and compound 4 oriented the 3,4-dihydroxyphenyl group towards the active site in an orientation similar to the pharmacological inhibitor acarbose. Nevertheless, the first-rank docking pose of α-14 was different compared to the other three inhibitors and acarbose. The α-14 inhibitor was bound to the enzyme in an opposite side with respect to the 3,4-dihydroxyphenyl group. This is not surprising because the bound side of α-14 shares similar chemical composition and structural shape compared to the dihydroxylphenyl group. Therefore, residues that are responsible for the binding, were not experienced different interactions with the α-14 inhibitor. It should be noted that a similar binding oritentation of the α-14 inhibitor was found in the second-rank docking pose. It is, therefore, the binding pose of the second rank was also taken into consideration for further MD study. This system is denoted as α-14* (Figure 3.2).

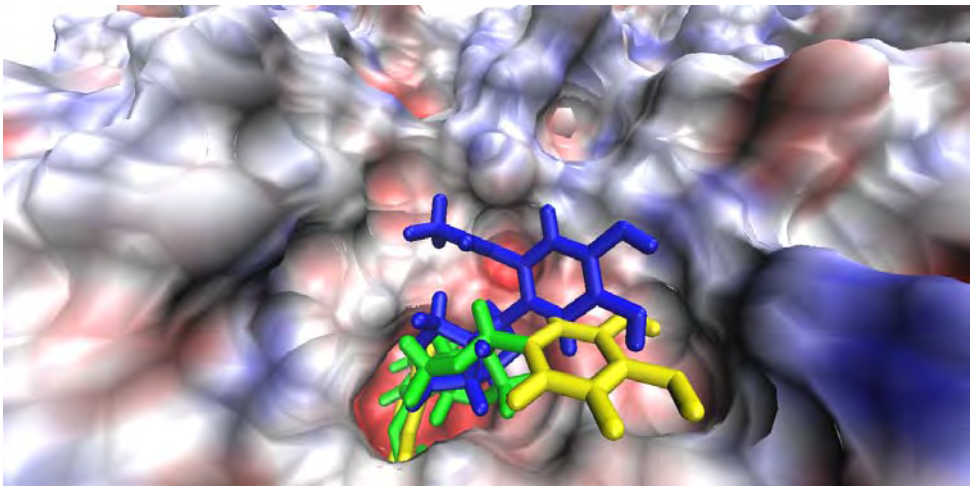

Figure 3.2 The docking pose of the first (green stick) and second (blue stick) ranks of the α-14 compound in the enzyme binding site (molecular surface colored based on electrostatic potential). The 3,4-dihydroxyphenyl ring is shown in yellow.

3.2 Assessment of the docking pose by MD simulations

Table 3.1 The simulated systems for MD simulation. The suffix -W is the system that included water molecule from the crystal structure.

System	ligand	Crystal water	Box size (Å^3)	Total number of atoms
acarbose	acarbose	-	130x130x130	204,735
α-8b	α-8b	-	130x130x130	204,695
α-14	α-14	-	130x130x130	204,714
β-14	β-14	-	130x130x130	204,708
4	compound 4	-	130x130x130	204,696
α-14*	The second lowest docking energy of α-14	-	130x130x130	204,717
acarboseW	acarbose	✓	130x130x130	205,074
α-8bW	α-8b	✓	130x130x130	205,052
α-14*W	The second lowest docking energy of α-14	✓	130x130x130	205,059
β-14W	β-14	✓	130x130x130	205,038
4W	compound 4	✓	130x130x130	205,047

3.2.1 Stability of inhibitors without crystallographic waters

MD simulations of the protein-inhibitor complex were carried out to assess the binding pose predicted by the docking method. The 100ns simulations were sufficiently long for monitoring the stability of inhibitors in the binding site. The root mean square deviation (RMSD) plot of protein backbone or ligands as a function of time was used to illustrate structure fluctuation with respect to the starting structure. The RMSD of protein backbone and ligand atoms from the simulation without incorporating crystal waters were shown in Figure 3.3. The protein backbone RMSD values during the last 20 ns of the simulations of the crystal water-excluded systems were 1.88±0.08, 1.89±0.13, 1.69±0.14, 1.78±0.22, 1.83±0.09, 1.70±0.13 Å deviating from the starting structure. The obtained RMSD values were small, indicating a small deviation of the global protein structure compared to the x-ray structure. This suggested that the absence of crystal waters has no significant effect on the overall tertiary structure of the protein. In contrast, it appears that the structure fluctuation of all inhbitors was remarkably large, including acarbose, the know x-ray structure (the control system). The RMSD values of all inhibitors during the 80-100ns simulation time were in a range from 5 to 25Å with respect to the starting structure of the simulation (the docking pose). This indicated that the inhibitors were unstable in the binding pocket.

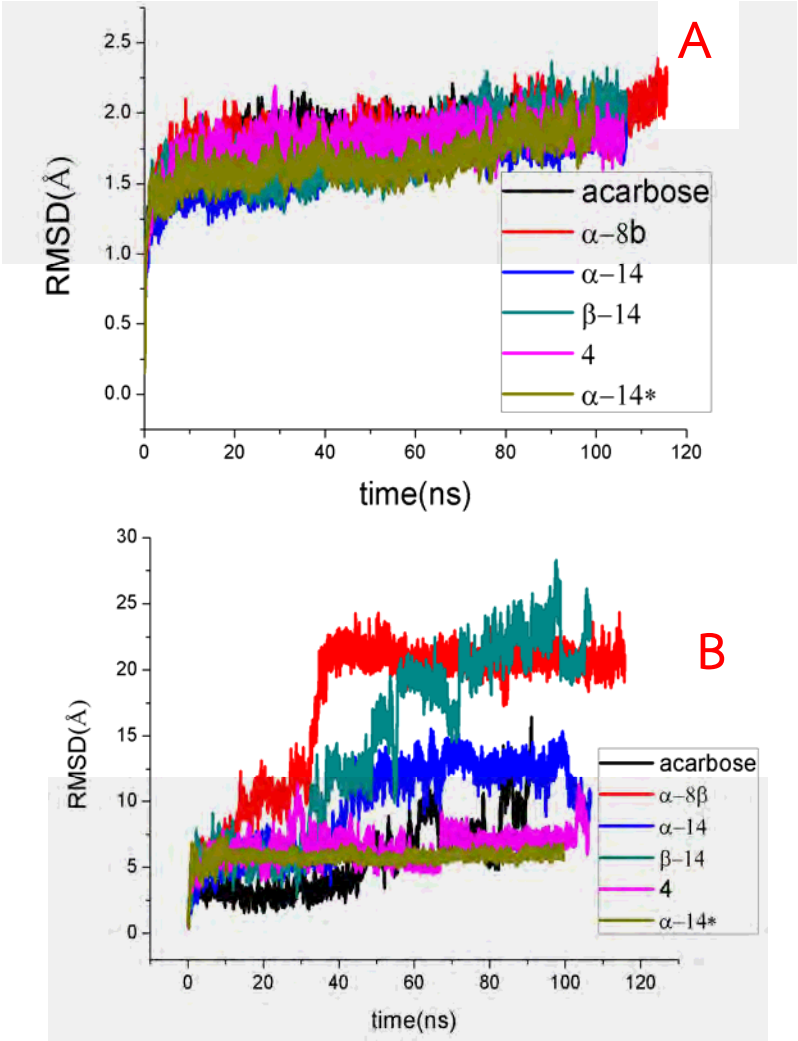

Figure 3.3 RMSD with respect to the starting structure versus the simulation time. The RMSD for protein backbone (A) and inhibitors (B). The **α**-14* system is the second lowest docking energy of **α**-14 inhibitor.

3.2.2 Stability of inhibitors with crystallographic waters

The systems were prepared by including atomic coordinates of all waters present in the crystallographic data (2QMJ). The RMSD plots for protein backbone and inhibitors are shown in Figure 3.4. The average RMSD of protein backbone atoms during the last 20 ns of the simulation time were 2.29±0.16, 2.13±0.13, 1.99±0.14, 1.99±0.13 1.82±0.16 Å for the systems containing acarbose, **α**-8b, **α**-14*, **β**-14, compound 4 systems, respectively. This suggested the overall tertiary structure of the protein remained unchanged compared to the x-ray structure. As expected, the tertairy structure of the protein has not been affected by

interactions with the crystal waters as has previously been discussed. A role of crystallographic water is clearly seen from an RMSD analysis of the inhibitors. In comparison with the crystal water-excluded simulation, structure fluctuation of acarbose , α-8b, α-14*, β-14, compound 4 systems were much smaller with the average RMSD values of 3.02±0.40, 2.46±0.40, 3.44±0.48, 3.87±0.37, 4.47±1.15 Å, respectively. However, the compound 4 system seems to be out of the binding pocket. Altogether, the results suggested that the inhibitors were found to be more stable in the binding pocket.

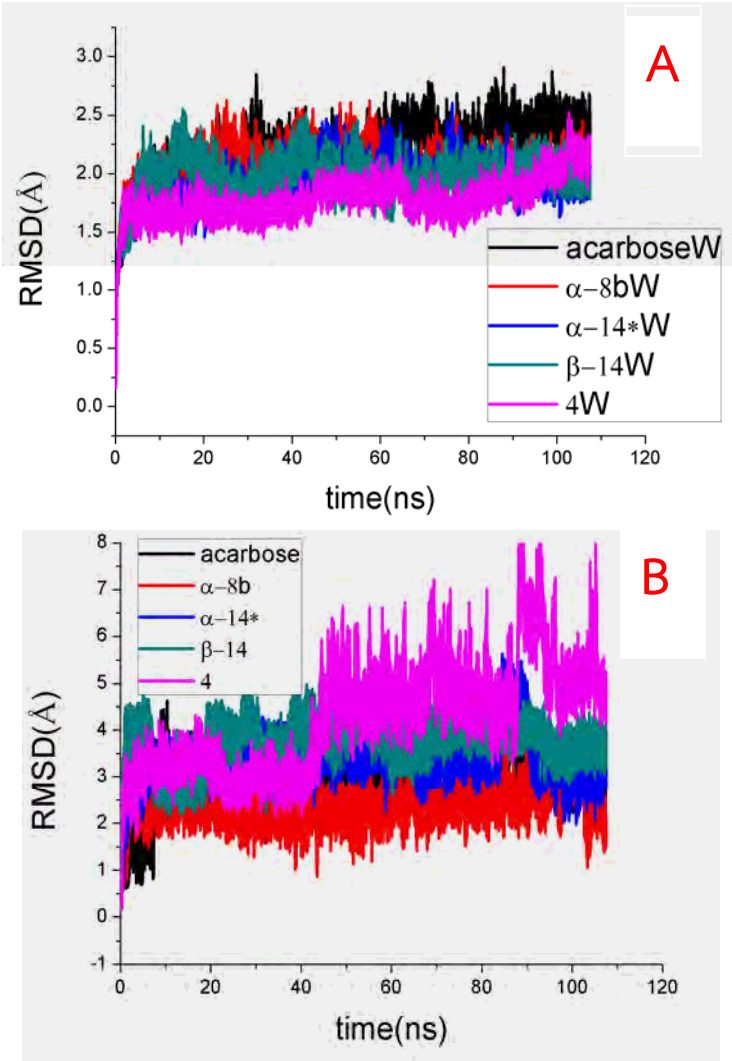

Figure 3.4 RMSD with respect to the starting structure versus the simulation time. The RMSD computed using protein backbone (A) and ligand (B). The α-14*W system is the second lowest docking energy of α-14 inhibitor.

3.2.2 Hydrogen bond (H-bond) analysis

The hydrogen bond is major intermolecular interaction between ligand and protein. Amino acid residues that possibly form a hydrogen bond with inhibitors are summarized in Table 3.1 and Figure 3.4. From the result, the number of hydrogen bonds for compound 4 was found to be the lowest. As shown in Table 3.1, enzyme-inhibitor interactions in terms of the number of H-bonds in five complexes were found to be in the following order: maltase-acarbose > maltase-α-14 = maltase-β-14 > maltase-α-8b > maltase-compound 4. Amino acid residues that were identified to interact with the inhibitors include TYR299, ASP327, ILE328, ILE364, TRP406, IRP441, ASP443, PHE450, ARG526, ASP542. Compound 4 appeared to interact with residues outside the the active site. From Figure 3.4, the 3,4-dihydroxyphenyl group of furofuran lignans was found to be an important part for interactions with the enzyme maltase. The difference between binding mode of α-stereoisomer and β-stereoisomer is 3,4-dihydroxyphenyl part binding amino acid residue. The 3,4-dihydroxyphenyl of α-stereoisomer binds with ASP327 residue and β-stereoisomer binds with ASP443.

Table 3.2 The hydrogen bond result between human maltase and each inhibitor.

compound	Number of Possible H-bond	H-bond interacting residue
Acarbose	8	ASP443, ASP542, HIS600, GLN603, TYR605
α-8b	4	THR205, ASP327, TYR605
α-14	5	TYR299, TRP406, ASP443, GLN603
β-14	5	TYR299, ASP327, ARG598
4	2	GLU300

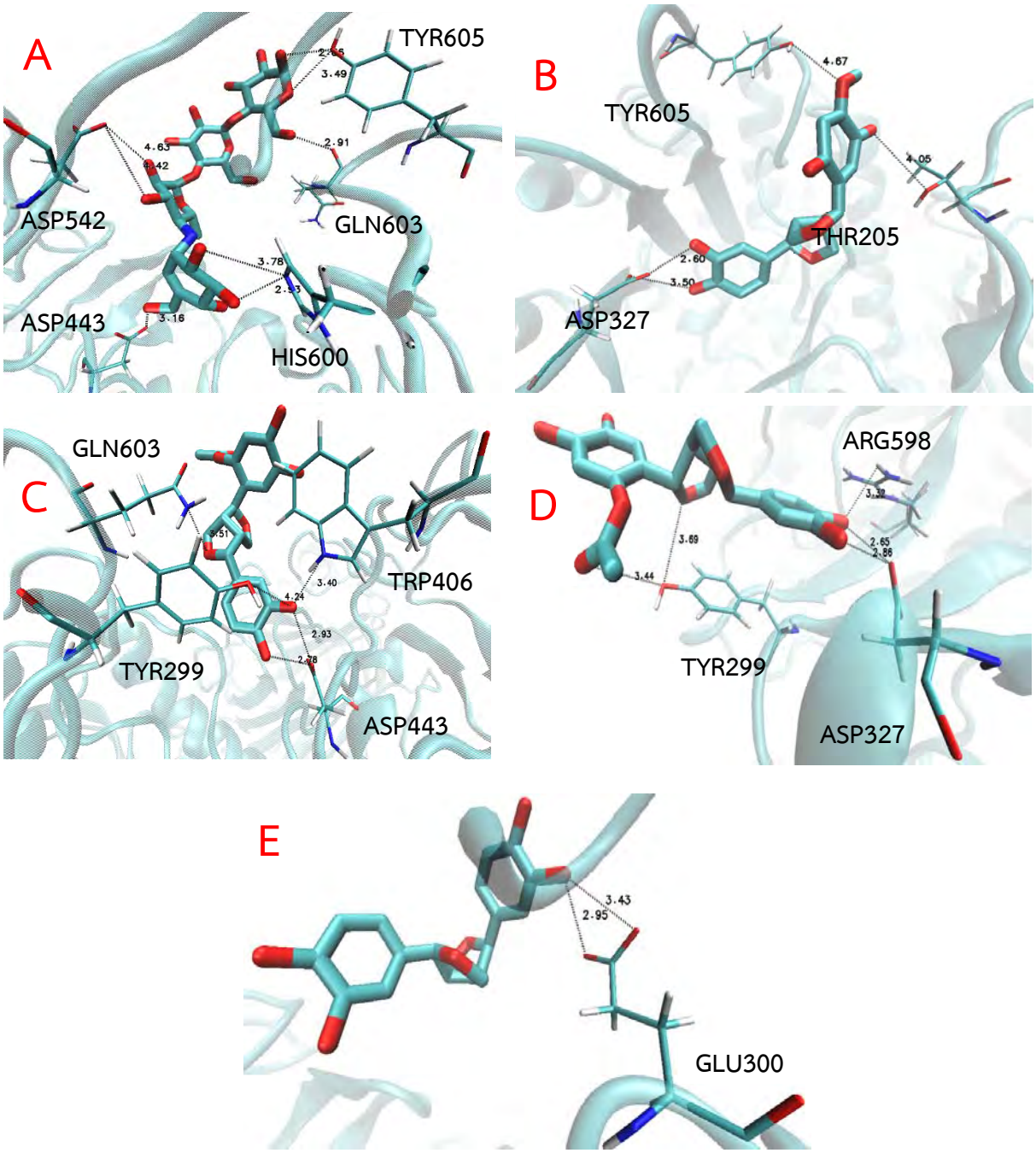

Figure 3.5 The possible hydrogen bond of human maltase and acarbose (A), **α**-8b (B), **α**-14 (C), **β**-14 (D), compound 4 (E).

3.2.3 Free energy analysis of enzyme-inhibitor binding

The binding free energy of the enzyme-inhibitor complex was calculated using MM-GBSA approach. The binding free energy of four systems (excluding maltase-compound 4) are shown in Table 3.3. As shown in Table 3.3, the negative free energies of all the complexes suggested the binding of the inhibitors is favorable. The calculated results showed that the order of ΔG_{bind} is maltase-**β**-14 > maltase-**α**-14 > maltase-acarbose > maltase-**α**-8b, which is consistent with the order of the experimental IC_{50} values (Table 3.3), except for acarbose.

Table 3.3 The prediction binding free energy between protein and each inhibitor and The experimental value of half maximal inhibitory concentration (IC_{50}) of each inhibitor with rat intestinal maltase.

compound	Binding free energy (kcal/mol)	IC_{50}* (μM)
acarbose	-16.01±4.07	1.40±0.2
α-8b	-11.56±4.10	97.0±1.2
α-14	-18.06±2.53	38.8±1.0
β-14	-20.99±4.00	25.7±1.0

* experiment value, rat intestinal maltase

Chapter 4

CONCLUSION

Interactions between human maltase and furofuran ligands inhibitors, namely α-8b, α-14, β-14 and compound 4, were investigated using molecular docking and molecular dynamics simulations. Molecular docking results showed that all furofuran lignans were bound in the active site of the enzyme with a very similar binding pose. α-8b, β-14 and compound 4 were oriented in such a way that the 3,4-dihydroxyphenyl group faces towards the active site similar to the pharmacological inhibitor acarbose. The MD study showed that the crystal water enhance the stability of the inhibitors in the binding pocket. Based on the number of H-bonds, enzyme-inhibitor interactions of five complexes were found to be in the following order: maltase-acarbose > maltase-α-14 = maltase-β-14 > maltase-α-8b > maltase-compound 4. Except for acarbose and compound 4, the order of binding free energy is maltase-β-14 > maltase-α-14 > maltase-α-8b, which is consistent with the order of the experimental data.

REFERENCES

1. Skyler, J. S., Diabetes mellitus: pathogenesis and treatment strategies. *Journal of Medicinal Chemistry* **2004,** *47* (17), 4113-4117.

2. Ingle, P. V.; B, Y. S.; Ying, B. J.; Leong, B. K.; Xin, T. Z.; Hwa, L. T.; Mun, L. T., Current Trends in Pharmacological Treatment of Type II Diabetes Mellitus *International Journal of Pharmacy Review and Research* **2018,** *7* (1), 1-15.

3. Chaudhuri, A.; Dandona, P., Effects of insulin and other antihyperglycaemic agents on lipid profiles of patients with diabetes. *Diabetes, Obesity and Metabolism* **2011,** *13* (10), 869-879.

4. Tuomi, T., Type 1 and type 2 diabetes: what do they have in common? *Diabetes* **2005,** *54* (suppl 2), S40-S45.

5. Costanian, C.; Bennett, K.; Hwalla, N.; Assaad, S.; Sibai, A. M., Prevalence, correlates and management of type 2 diabetes mellitus in Lebanon: findings from a national population-based study. *Diabetes research and clinical practice* **2014,** *105* (3), 408-415.

6. Olokoba, A. B.; Obateru, O. A.; Olokoba, L. B., Type 2 diabetes mellitus: a review of current trends. *Oman medical journal* **2012,** *27* (4), 269.

7. Wu, Y.; Ding, Y.; Tanaka, Y.; Zhang, W., Risk factors contributing to type 2 diabetes and recent advances in the treatment and prevention. *International Journal of Medical Sciences* **2014,** *11* (11), 1185.

8. Saeedi, P.; Petersohn, I.; Salpea, P.; Malanda, B.; Karuranga, S.; Unwin, N.; Colagiuri, S.; Guariguata, L.; Motala, A. A.; Ogurtsova, K., Global and regional diabetes prevalence estimates for 2019 and projections for 2030 and 2045: Results from the International Diabetes Federation Diabetes Atlas. *Diabetes research and clinical practice* **2019,** *157*, 107843.

9. Krentz, A. J.; Bailey, C. J., Oral antidiabetic agents. *Drugs* **2005,** *65* (3), 385-411.

10. Eun, H.-M., *Enzymology primer for recombinant DNA technology*. Elsevier: 1996.

11. Trapero, A.; Llebaria, A., A prospect for pyrrolidine iminosugars as antidiabetic α-glucosidase inhibitors. *Journal of Medicinal Chemistry* **2012,** *55* (23), 10345-10346.

12. de Melo, E. B.; da Silveira Gomes, A.; Carvalho, I., α-and β-Glucosidase inhibitors: chemical structure and biological activity. *Tetrahedron* **2006,** *62* (44), 10277-10302.

13. Pullela, S. V.; Tiwari, A. K.; Vanka, U. S.; Vummenthula, A.; Tatipaka, H. B.; Dasari, K. R.; Khan, I. A.; Janaswamy, M. R., HPLC assisted chemobiological standardization of α-glucosidase-I enzyme inhibitory constituents from Piper longum Linn-An Indian medicinal plant. *Journal of ethnopharmacology* **2006,** *108* (3), 445-449.

14. Kim, J.-S.; Kwon, C.-S.; SoN, K. H., Inhibition of alpha-glucosidase and amylase by luteolin, a flavonoid. *Bioscience, biotechnology, and biochemistry* **2000,** *64* (11), 2458-2461.

15. Pohmakotr, M.; Kuhakarn, C.; Reutrakul, V.; Soorukram, D., Asymmetric synthesis of furofurans. *Tetrahedron Letters* **2017,** *58* (51), 4740-4746.

16. Worawalai, W.; Doungwichitrkul, T.; Rangubpit, W.; Taweechat, P.; Sompornpisut, P.; Phuwapraisirisan, P., Furofuran lignans as a new series of antidiabetic agents exerting α-glucosidase inhibition and radical scarvenging: Semisynthesis, kinetic study and molecular modeling. *Bioorganic chemistry* **2019,** *87*, 783-793.

17. Andrew, R. L., Molecular modeling principles and applications. *Prentice Hall, London* **2001**.

18. González, M., Force fields and molecular dynamics simulations. *École thématique de la Société Française de la Neutronique* **2011,** *12*, 169-200.

19. Monticelli, L.; Tieleman, D. P., Force fields for classical molecular dynamics. In *Biomolecular simulations*, Springer: **2013**, 197-213.

20. Lindahl, E.; Hess, B.; Van Der Spoel, D., GROMACS 3.0: a package for molecular simulation and trajectory analysis. *Molecular modeling annual* **2001,** *7* (8), 306-317.

21. van der Spoel, D.; Lindahl, E.; Hess, B.; Van Buuren, A.; Apol, E.; Meulenhoff, P.; Tieleman, D.; Sijbers, A.; Feenstra, K.; van Drunen, R., Gromacs user manual version 3.2. *Nijenborgh* **2004,** *4*, 9747.

22. Ribeiro, J. V.; Cerqueira, N. M.; Moreira, I. S.; Fernandes, P. A.; Ramos, M. J., CompASM: an Amber-VMD alanine scanning mutagenesis plug-in. *Theoretical Chemistry Accounts* **2012,** *131* (10), 1271.

23. Humphrey, W.; Dalke, A.; Schulten, K., VMD: visual molecular dynamics. *Journal of molecular graphics* **1996,** *14* (1), 33-38.

24. Hsin, J.; Arkhipov, A.; Yin, Y.; Stone, J. E.; Schulten, K., Using VMD: an introductory tutorial. *Current protocols in bioinformatics* **2008,** *24* (1), 5.7. 1-5.7. 48.

25. Kalé, L.; Skeel, R.; Bhandarkar, M.; Brunner, R.; Gursoy, A.; Krawetz, N.; Phillips, J.; Shinozaki, A.; Varadarajan, K.; Schulten, K., NAMD2: greater scalability for parallel molecular dynamics. *Journal of Computational Physics* **1999,** *151* (1), 283-312.

26. MacKerell Jr, A. D.; Brooks, B.; Brooks III, C. L.; Nilsson, L.; Roux, B.; Won, Y.; Karplus, M., CHARMM: the energy function and its parameterization. *Encyclopedia of computational chemistry* **2002**.

27. Sim, L.; Quezada-Calvillo, R.; Sterchi, E. E.; Nichols, B. L.; Rose, D. R., Human intestinal maltase–glucoamylase: crystal structure of the N-terminal catalytic subunit and basis of inhibition and substrate specificity. *Journal of molecular biology* **2008,** *375* (3), 782-792.

APPENDIX

Appendix I: Show example input file for Molecular Dynamic simulation

```
paraTypeCharmm       on
parameters ../par_all36m_prot.prm
parameters ../par_all36_cgenff.prm
parameters ../lig.prm
parameters ../water-mod.prm

# Force-Field Parameters
exclude              scaled1-4
1-4scaling           1.0
cutoff               12.0
switching            on
switchdist           10.
pairlistdist         13.5

#PME (for full-system periodic electrostatics)
if {1} {PME                  yes
PMEGridSizeX         130
PMEGridSizeY         130
PMEGridSizeZ         130 }

# Integrator Parameters
timestep             2.0   ;# 2fs/step
rigidBonds           all  ;# needed for 2fs steps
nonbondedFreq        1
fullElectFrequency   2
stepspercycle        20
```

```
# Constant Temperature Control
if {$temode == "t"} {
langevin            yes  ;# do langevin dynamics
langevinDamping     1     ;# damping coefficient(gamma)5/ps
langevinTemp        $temperature
langevinHydrogen    off    ;# don't couple langevin bath to hydrogens }

# Periodic Boundary Conditions
if {1} { cellBasisVector1    130.0     0.0     0.0
cellBasisVector2     0.0     130.0    0.0
cellBasisVector3     0.0      0.0     130.0
cellOrigin           0.0   0.0   0.0}
wrapAll              on
wrapWater            on

# Constant Pressure Control (variable volume)
useGroupPressure      no
useFlexibleCell       no    ;# no for water box, yes for membrane
useConstantArea       no    ;# no for water box, yes for membrane
if {$pvmode == "p"} {
langevinPiston        on
langevinPistonTarget  1.01325 ;#  in bar -> 1 atm
langevinPistonPeriod  200.  #usually 2000 for RBCG
langevinPistonDecay   50.  #usually 1000 for RBCG
langevinPistonTemp    $temperature #set temperature 298}
# Heating
reassignFreq    2000
reassignTemp    100
reassignIncr    1
reassignHold    $temperature
```

VITAE

MR. Pisit Lerttanakij born on 15th October 1997 at Bangkok. I graduated high school from The Secondary Demonstration School of Bansomdejchaopraya Rajabhat University in 2015. After that, I continued his study in Department of Chemistry, Faculty of Science, Chulalongkorn University in 2016. I got scholarship from The Development and Promotion of Science and Technology Talents Project (DPST) since 2016. The present address after graduate: 5/163 soi Bangbon 5 soi 18 Bangbon 5 road, Bangbon, Bangbon district, Bangkok 10150. Email: basspisit@gmail.com